

## The Effect of TiO<sub>2</sub> Thin Films Produced in Different Thicknesses on Dye-Sensitized Solar Cell Performance

Fehmi ASLAN<sup>1\*</sup>

<sup>1</sup> Department of Motor Vehicles and Transportation Technologies, Yesilyurt Vocational School, Malatya Turgut Ozal University, Malatya, Türkiye  
\*<sup>1</sup> fehmi.aslan@ozal.edu.tr

(Geliş/Received: 08/05/2023;

Kabul/Accepted: 24/08/2023)

**Abstract:** Dye-sensitized solar cells (DSSC) are known as 3rd generation solar cells. One of the most important parameters affecting the performance of DSSCs is the thin film thickness that forms the photoanode layer. In this study, we examined how 38, 60 and 76 µm thick TiO<sub>2</sub> thin films change dye-sensitized solar cell performance. The highest efficiency (4.73%) was seen in the solar cell with 38 µm thin film thickness. In addition, the mineralogical and morphological analyses of the produced TiO<sub>2</sub> nanopowders were performed with X-ray diffraction (XRD) and Scanning electron microscopy (SEM). XRD analyses showed that TiO<sub>2</sub> was in the anatase crystal phase. SEM photographs confirmed the formation of microspheres in close contact with each other.

**Keywords:** DSSC, photoanode, thin film thickness, cell performance.

### Farklı Kalınlıklarda Üretilen TiO<sub>2</sub> İnce Filmlerinin Boya Duyarlı Güneş Pili Performansına Etkisi

**Öz:** Boya duyarlı güneş pilleri (DSSC) 3. nesil güneş pilleri olarak bilinmektedir. DSSC'lerin performansını etkileyen en önemli parametrelerden birisi fotoanot katmanı oluşturan ince film kalınlığıdır. Bu çalışmada 38, 60 ve 76 µm kalınlığındaki TiO<sub>2</sub> ince filmlerinin boya duyarlı güneş pili performansını nasıl değiştirdiğini inceledik. En yüksek verimlilik (%4.73) 38 µm ince film kalınlığına sahip güneş pilinde görüldü. Ayrıca üretilen TiO<sub>2</sub> nanotozlarının mineralojik ve morfolojik analizleri X-ışını difraksiyonu (XRD) ve Taramalı elektron mikroskobu (SEM) ile gerçekleştirildi. XRD analizleri TiO<sub>2</sub>'nin anataz kristal fazında olduğunu gösterdi. SEM fotoğrafları ise birbirine yakın temasta mikrokürecik yapıların oluşumunu doğruladı.

**Anahtar kelimeler:** DSSC, fotoanot, ince film kalınlığı, hücre performansı.

#### 1. Introduction

Today, our lives are getting easier thanks to technological developments that are gaining momentum very quickly. The new inventions that human beings add to our lives play a major role in increasing our quality of life. Every building that provides convenience for our comfort is fed from an energy source [1]. To meet this energy need, exhaustible, renewable and nuclear energy sources are used today [2].

Since the electrical energy produced by solar energy is renewable, environmentally friendly and will continue to exist as long as the world exists, its usage areas are very wide. For this reason, it is thought that solar energy will play a major role in solving the energy problem, which is one of the biggest problems of humanity. Another factor that makes solar energy important is that it is a renewable energy source, does not pose any danger and is environmentally friendly. Since solar energy is an energy source that all human beings need, it requires extensive research in reducing energy dependence [3,4].

Dye-sensitized solar cells (DSSCs), like other solar cells, work with the principle of converting light into electrical energy. A typical DSSC consists of a photoanode, dye, redox electrolyte and counter electrode to catalyze the reaction [5]. They are formed by dipping the semiconductor metal oxide material coated on a conductive glass surface into the dye and then joining it with the counter electrode after pouring the electrolyte solution. The schematic structure of a typical DSSC is given in Fig. 1. More research is needed to increase the commercial use of DSSCs and to transform this technology into a more competitive product in the world market. To increase commercial production, it is necessary to obtain an efficiency of more than 15% from DSSCs [6]. Researchers have worked to increase the power conversion efficiency of DSSCs by producing dyes with high extinction coefficients, metal oxide photoanodes with increased specific surface area, new redox electrolytes and counter electrodes [7,8].

\* Corresponding author: fehmi.aslan@ozal.edu.tr. ORCID Number of authors: 0000-0002-5304-0503

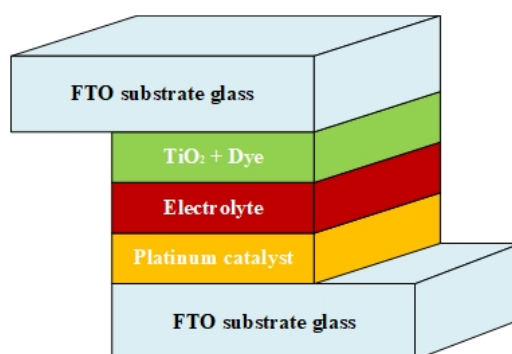


**Figure 1.** Schematic structure of a typical DSSC [9].

In addition to the morphological and electronic structure of TiO<sub>2</sub>, the film thickness also significantly affects cell performance. Most of the cracks and shrinkage in the TiO<sub>2</sub> layer are related to the layer thickness. Cracks seen in the thin film layer slow down electron transport, cause a short circuit and reduce the active surface area [10]. For this reason, the thickness of the TiO<sub>2</sub> layer of DSSC should be optimized. In a study by Kao et al., when TiO<sub>2</sub> thin films of different thicknesses (0.5 μm, 1 μm, 1.5 μm and 2 μm) were examined, an increase of 5% in the short circuit current density and open circuit voltage of DSSC with 1.5 μm thin film thickness was observed [11]. The cell with 10 μm TiO<sub>2</sub> film exhibited the highest light absorption and lowest charge recombination among photoanodes with layers of different thicknesses (6, 10 and 14 μm) [12]. When the layer thickness exceeds 15 μm, photovoltaic parameters such as power conversion efficiency and short-circuit current density decrease [13]. In previous studies, it is known that the performance of DSSCs decreases when the thin film thickness reaches around 15 μm. Especially when the film thickness exceeds 15 μm, it is known that there is a great decrease in productivity. In this study, it was investigated how the photovoltaic parameters were affected by using thicker films.

In this study, the extent to which higher film thicknesses affect the performance of DSSCs was investigated. For this purpose, TiO<sub>2</sub> layers with 38, 60 and 76 μm thickness were produced.

## 2. Experiments

All chemical materials required for this study were purchased commercially and used without further purification. All experiments were carried out in sterile conditions in a laboratory environment.

### 2.1 Materials used in the experiment

In this study; Titanium IV isopropoxide (TTIP, ≥97.0%, Sigma-Aldrich), ethyl alcohol (≥99.5%, Sigma-Aldrich), ethyl cellulose (Sigma-Aldrich), alpha-terpinol (Sigma-Aldrich), acetone (99.5%, Sigma-Aldrich), Fluorine doped tin oxide coated glass (FTO, surface resistivity approximately 13 Ω/sq), Electrolyte solution (Iodolyte AN-50, Solaronix) and Platinum (Pt) paste (Solaronix) were used.

### 2.2 Production of titanium dioxide (TiO<sub>2</sub>) nanoparticles

In this study, the hydrothermal system shown in Fig. 2 was used for the production of TiO<sub>2</sub> nanopowders. Initially, 40 ml of deionized water and 1.6 g of urea were mixed for 1 h until a homogeneous solution was formed. While this process was continuing, 3.5 ml of TTIP was added dropwise and mixed for another 30 min. After this mixture was ultrasonically treated for 30 min, it was placed in a Teflon autoclave integrated hydrothermal device at 120 °C for 24 h. After the Teflon autoclave was cooled to room temperature, the collected particles were washed several times with deionized water and alcohol to remove unwanted residues. The precipitate formed was dried in an oven at 50 °C for 12 h and calcined in a muffle furnace at 450 °C. Produced TiO<sub>2</sub> particles were pounded in a mortar and made ready for paste making.



Figure 2. Hydrothermal system used in nanopowder production.

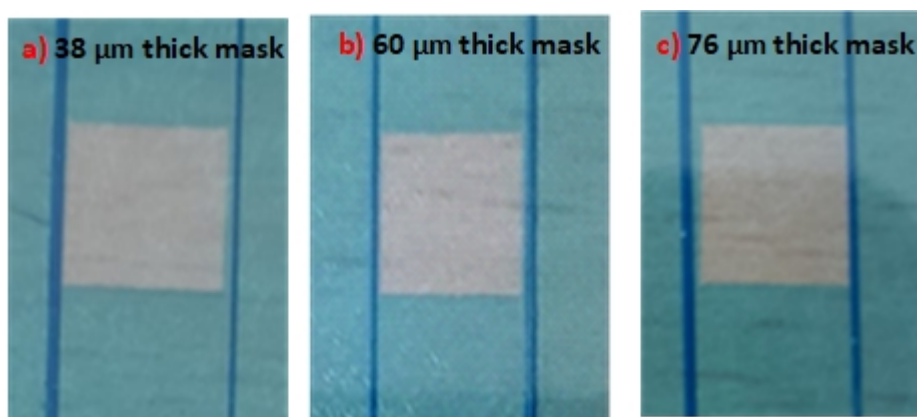
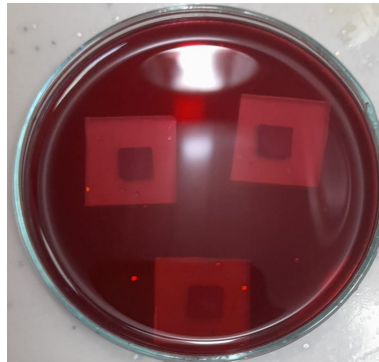


Figure 3. Masks of different thicknesses are pasted on the FTO.

### 2.3. Preparation of DSSCs

To prepare the paste, 2 g of  $\text{TiO}_2$ , 0.9 g of ethyl cellulose and 6 ml of terpinol were mixed in a mortar until the appropriate paste concentration was obtained. Non-marking masking tapes with 38, 60 and 76  $\mu\text{m}$  thickness and  $0.6 \text{ cm} \times 0.6 \text{ cm}$  opening adhered to the  $2 \text{ cm} \times 2 \text{ cm}$  FTO conductive glass surface. Masks pasted on the FTO are shown in Fig. 3. The pre-prepared  $\text{TiO}_2$  paste was coated with a doctor-blade technique on the conductive surface of the FTOs with the help of a glass rod. The produced photoanodes were calcined at  $450 \text{ }^\circ\text{C}$  for 45 min with gradual heating. After cooling the photoanodes at room temperature, they were immersed in 0.5 mM Ru dye dissolved in anhydrous alcohol and kept in a dark environment for 24 h. The photoanodes immersed in dye are given in Fig. 4. Photoanodes removed from the dye were washed several times with alcohol to remove non-absorbable residues on the surface and quickly dried. To produce Pt counter electrodes, Pt-based paste was coated on the conductive surface of the FTO with the help of an acrylic brush. FTO coated with Pt paste was sintered at  $450 \text{ }^\circ\text{C}$  for 15 min and counter electrodes were prepared. After a few drops of electrolyte solution was dropped on the part where  $\text{TiO}_2$  was located on the photoanode layer, it was combined with the Pt counter electrode. After this process, the DSSCs are ready to take measurements. The representative view of the prepared DSSCs is given in Fig. 5.



**Figure 4.** The appearance of photoanodes with different thicknesses in Ru dye.



**Figure 5.** The representative view of the prepared DSSCs

### 3. Discussion and results

The XRD patterns of the produced TiO<sub>2</sub> nanopowders are given in Fig. 6. XRD measurements were performed at 2 $\theta$  angles from 10° to 80°. XRD analyses (performed by the Rigaku X-ray Diffraction system) confirmed the high-quality crystal structure and anatase phase of TiO<sub>2</sub>. In addition, (101), (004), (200), (105), (211), (204), (116), (220), (215) XRD crystal planes overlap the 2 $\theta$  angles of anatase TiO<sub>2</sub> [14].

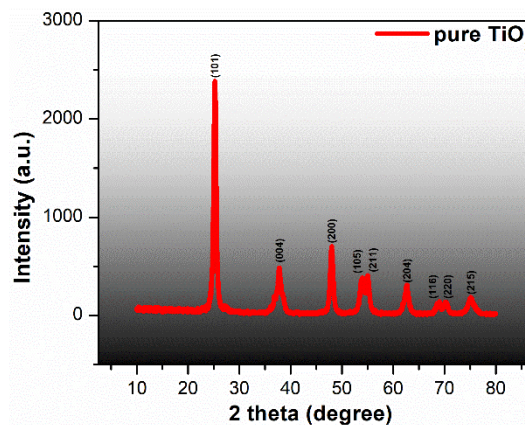


**Figure 6.** XRD patterns of produced TiO<sub>2</sub> particles.

The surface morphology of TiO<sub>2</sub> powders produced by the hydrothermal method was examined by SEM analysis (performed by ZEISS Sigma-300). The surface morphologies of TiO<sub>2</sub> particles are given in Fig. 7. The particles were composed of tightly packed microspheres, and this tight contact facilitated electron transport.

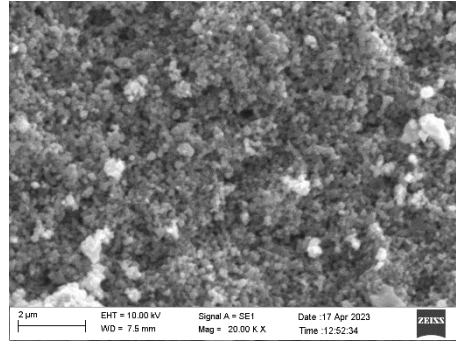


Figure 7. SEM images of the produced TiO<sub>2</sub> particles.

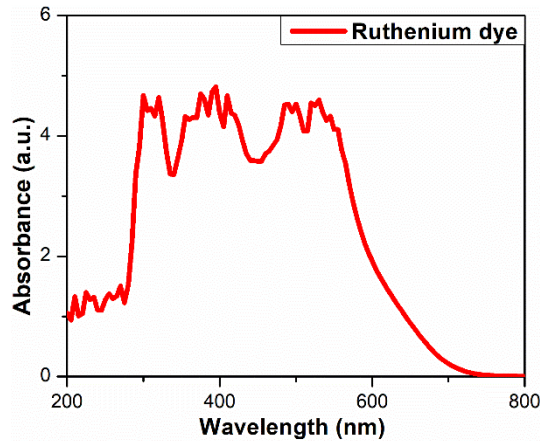


Figure 8. UV-vis spectrum of ruthenium-based dye.

Photoanodes with TiO<sub>2</sub> layers of different thicknesses were immersed in a Ru-based dye solution, which showed the highest cell performance for DSSCs. The UV-vis absorption spectrum lines of the Ru dye are shown in Fig. 8. Thanks to the high absorption of Ru-based dye in the wavelength range of 340-760 nm, DSSCs with 38, 60 and 76 μm TiO<sub>2</sub> layer thicknesses showed photoelectric conversion efficiency ( $\eta$ ) of 4.73%, 3.89% and 3.82%, respectively.

Photovoltaic parameters and charge transfer properties of the produced DSSCs were recorded by the Fytronix Solar Simulator LSS 9000 I-V Characterization System under simulated sunlight (AM1.5G, 100 mW/cm<sup>2</sup> light intensity, 1.0 Sun). Fig. 9 shows the J<sub>sc</sub>-V (short-circuit current density-voltage) curves of DSSCs with thin films of different thickness under 100 mW/cm<sup>2</sup> light intensity (AM1.5G). Photoelectric conversion efficiencies ( $\eta$ ) and filling factors (FF) of the produced cells are calculated by Eq. 1 and 2, respectively [12]. In these equations,  $\eta$  is the power conversion efficiency; P<sub>in</sub>, P<sub>max</sub>, J<sub>sc</sub>, and V<sub>oc</sub> represent input power, maximum power, short-circuit current density, and open-circuit voltage, respectively; V<sub>max</sub> and J<sub>max</sub> correspond to the maximum voltage and current density, respectively.

$$\eta = \frac{P_{\max}}{P_{in}} = \frac{V_{oc} \times J_{sc} \times FF}{P_{in}} \quad (1)$$

$$FF = \frac{J_{\max} \times V_{\max}}{J_{sc} \times V_{oc}} \times 100 \quad (2)$$

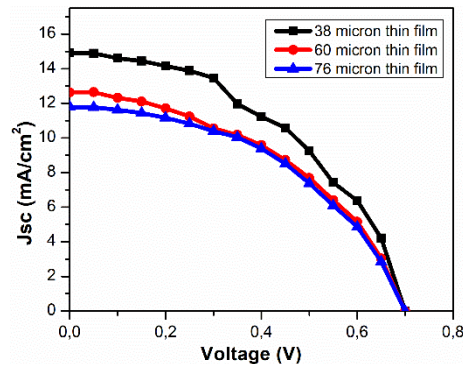


**Figure 9.** J<sub>sc</sub>-V curves of DSSCs with different TiO<sub>2</sub> thicknesses.

**Table 1.** Photovoltaic parameters of DSSCs.

Sample	J <sub>sc</sub> (mA/cm <sup>2</sup> )	V <sub>oc</sub> (V)	FF	η (%)
DSSC with 38 μm film thickness	14.92	0.64	0.47	4.73
DSSC with 60 μm film thickness	12.63	0.67	0.50	3.89
DSSC with 76 μm film thickness	11.78	0.64	0.49	3.82

When the photovoltaic parameters of the prepared DSSCs given in Table 1 were examined, the highest η (4.73%) and J<sub>sc</sub> value (14.92 mW/cm<sup>2</sup>) was seen in the cell with the thinnest layer of 38 μm. In addition, it has been determined that there is a decrease in η and J<sub>sc</sub> as the TiO<sub>2</sub> film thickness increases. This can be explained by low-charge recombination and high light absorption in cells with thinner layers [15]. Cracks may occur in the film layer, especially when the thin film thickness exceeds the optimized values. These cracks reduce power conversion efficiency and short-circuit current density [16].

#### 4. Conclusions

TiO<sub>2</sub> particles were produced by hydrothermal method and their mineralogical structures were confirmed by XRD. SEM images revealed tightly packed microsphere structures that facilitate electron transport. Terpinol and ethyl cellulose were used as binders in the paste prepared to produce the photoanodes. The doctor blending method was used to create a TiO<sub>2</sub> layer on FTO glasses. Among DSSCs with different thickness of TiO<sub>2</sub> layer, the cell with 38 μm film thickness exhibited the highest power conversion efficiency (4.73%) and short-circuit current density (14.92 mW/cm<sup>2</sup>). Higher-performance cells can be obtained by producing photoanodes with different layer thicknesses.

#### Declaration of Competing Interest

The authors declare that they have no known competing financial interests or personal relationships that could have appeared to influence the work reported in this paper.

#### Credit Authorship Contribution Statement

Fehmi Aslan: Conceptualization, Data curation, Formal analysis, Investigation, Methodology, Validation, Visualization, Writing – original draft, Writing - review & editing.

#### References

- [1] Bikçe M, Çelik AR, Çakır M. Investigation of solar energy efficiency in education laboratory: Case Study İskenderun. Cukurova University Journal of the Faculty of Engineering. 2016;31: 395–404.
- [2] Özgöçmen A, Electricity generation using solar cells. MSc, Gazi University, Ankara, Turkey, 2007.
- [3] Hernandez RR, Hoffacker CB. Efficient use of land to meet sustainable energy needs. Nat. Clim. Change. 2015;5: 353–358.
- [4] Zatirostami A. A dramatic improvement in the efficiency of TiO<sub>2</sub>-based DSSCs by simultaneous incorporation of Cu and Se into its lattice. Opt. Mater. 2021;117: 110-111.
- [5] Chu L, Qin Z, Zhang Q, Chen W, Yeng J, Yang J, Li X. Mesoporous anatase TiO<sub>2</sub> microspheres with interconnected nanoparticles delivering enhanced dye-loading and charge transport for efficient dye-sensitized solar cells. Appl. Surf.

- Sci. 2016;360: 634–640.
- [6] Eden Ç, Characterization and dye-sensitized solar cell performance of TiO<sub>2</sub>/ZnO nanocomposite structures synthesized at different temperatures. MSc, Erzincan Binali Yıldırım University, Erzincan, Turkey, 2019.
- [7] Xie Y, Huang N, You S, Liu Y, Sebo B, Liang L, Fang X, Liu W, et al. Improved performance of dye-sensitized solar cells by trace amount Cr-doped TiO<sub>2</sub> photoelectrodes, *J. Power Sources*. 2013;224: 168–173.
- [8] Qi K, Liu S, Chen Y, Xia B, Li GD. A simple post-treatment with urea solution to enhance the photoelectric conversion efficiency for TiO<sub>2</sub> dye-sensitized solar cells. *Sol. Energy Mater. Sol. Cells*. 2018;183: 193–199.
- [9] Supriyanto A, Nurosyid F, Ahliha AH. Carotenoid pigment as sensitizers for applications of the dye-sensitized solar cell (DSSC). *IOP Conf. Ser. Mater. Sci. Eng.* 2018;432: 012060.
- [10] Hossain MK, Rahman MT, Basher MK, Manir MS, Bashir MS. Influence of thickness variation of gamma-irradiated DSSC photoanodic TiO<sub>2</sub> film on structural, morphological and optical properties. *Opt*. 2019;178: 449–460.
- [11] Kao MC, Chen HZ, Young SL, Kung CY, Lin CC. The effects of the thickness of TiO<sub>2</sub> films on the performance of dye-sensitized solar cells. *Thin Solid Films*. 2009;517: 5096–5099.
- [12] Selyanin IO, Steparuk AS, Irgashev RA, Mekhaev AV, Rusinov GL, Vorokh AS. TiO<sub>2</sub> paste for DSSC photoanode: Preparation and optimization of application method. *Chim. Tech. Acta*. 2020;7(4): 140–149.
- [13] Fitra M, Daut I, Irwanto M, Gomes N, Irwan YM. Effect of TiO<sub>2</sub> thickness dye solar cell on charge generation. *Energy Procedia*. 2013;36: 278–286.
- [14] Xu J, Wang G, Fan J, Liu B, Cao S, Yu J. G-C<sub>3</sub>N<sub>4</sub> modified TiO<sub>2</sub> nanosheets with enhanced photoelectric conversion efficiency in dye-sensitized solar cells. *J. Power Sources*. 2015; 274: 77–84.
- [15] Baglio V, Girolamo M, Antonucci V, Aricò AS. Influence of TiO<sub>2</sub> film thickness on the electrochemical behavior of dye-sensitized solar cells. *Int. J. Electrochem. Sci*. 2011;6: 3375–3384.
- [16] Kumari J, Sanjeevadarshini N, Dissanayake M, Senadeera G, Thotawatthage C. The effect of TiO<sub>2</sub> photoanode film thickness on photovoltaic properties of dye-sensitized solar cells. *Ceylon J. Sci*. 2016;45: 33.